Research Article

Journal of Environmental Nanotechnology

Enhancing the Surface Quality and Tool Life Using Nano MQL-assisted Machining Characteristics of Aluminium Composite

M. Vivekanandhan[1], S. Gowtham[2], V. Senthil[2*] and C. Dhanesh[3]

[1]Department of Mechanical Engineering, Adhiparasakthi Engineering College, Melmaruvathur, TN, India
[2]Department of Mechanical Engineering, Government College of Engineering, Bodinayakanur, TN, India
[3]Department of Mechanical Engineering, S.A. Engineering College, Chennai, TN, India
Received: 20.11.2024 Accepted: 18.02.2025 Published: 30.03.2025
*senthilgcebn@gmail.com

ABSTRACT

This study investigates the effect of graphene nanoplatelets (GNPs) dispersed in minimum quantity lubrication (MQL) on turning performance of an aluminium composite. The composite consists of LM25 as the matrix and 10 wt.% of titanium carbide as reinforcement, fabricated *via* stir casting technique. Turning studies are performed on the turning center attached with MQL setup where different weight proportions of GNPs (1, 3, and 5 wt.%) are mixed with canola oil and supplied at the cutting zone. Experiments are designed by Taguchi's method, an appropriate L_9 orthogonal array is considered. The surface roughness (SR), and flank wear outcomes are measured and analyzed using grey relational analysis. Observation shows, the MQL consisting of 3 wt.% of GNPs provided lower Feed Force (FW) and SR as it lowers the interface temperature at cutting zone and easy dispersal of chips. Increases in FW and SR are mostly attributable to changes in the feed rate.

Keywords: Aluminium composite; Graphene; Minimum quantity lubrication; Flank wear; Surface roughness; Cutting zone.

1. INTRODUCTION

Machining aluminium composites reinforced with ceramic particles poses significant challenges owing to the ceramic reinforcement's abrasive and hard nature. During cutting, the interaction between the ceramic particles and the cutting tool generates high friction, leading to increased heat at the tool-workpiece interface (Nayak *et al*. 2022). This heat accelerates tool wear, particularly in conventional tools not designed for abrasive materials, resulting in rapid flank and crater wear. The hard particles can also chip or damage the cutting edge, reducing tool life and raising operational costs. Additionally, the uneven distribution of ceramic particles in the matrix often leads to inconsistencies in cutting force and cutting surface, which contributes to surface roughness and poor finish quality (Huo *et al*. 2021). The presence of ceramic particles makes it difficult to achieve fine surface finishes, as the particles tend to tear or plough through the matrix material, creating irregularities. These challenges necessitate careful selection of cutting tools (coated carbide or diamond tools), optimized cutting parameters, and effective cooling and lubrication techniques to reduce heat, minimize wear, and improve surface finish during the machining of these composites (Atkins 2009). The softening of the cutting tool at increased machining circumstances causes a link between cutting region temperature and flank wear. The most important component for cutting region temperature is nose radius, which in turn influences flank wear.

LM25+nSiC+MoS_2 composite was prepared by Raja *et al*. (2024) *via* ultrasonic assisted stir casting technique. It was found that higher quantities of nSiC produced higher strength and addition of MoS_2 influenced the mechanical strength of the hybrid composite considerably. The porosity decreases considerably with rise in density. Taguchi's technique was adopted for designing experiments and to optimize drilling parameters for lower thrust force and delamination. Drill diameter was shown to have the greatest impact on limiting thrust force, according to analysis of variance, whereas spindle speed was an extremely important component in lowering delamination. Machining studies on AA6061+ mica + boron carbide composite using response surface design was done and fuzzy logic was applied to enhance the quality of output and optimized the outputs using metaheuristic algorithm and desirability function. Outcome shows that the induced thrust force and torque decreased with rising spindle speed because of softening of matrix constituents (Kayaroganam *et al*. 2021).

Titanium carbide (TiC) has a high modulus of elasticity and outstanding compressive strength, which can enhance the stiffness and load-bearing capacity of aluminium composites. It aids in the synthesis of composites that are both lightweight and with very strong-to-weight ratio (Srinivasan *et al.* 2024). Researchers found that the crater and scratch are the main defects in the machined surface of direct energy deposited Ti6Al4V-titanium carbide composite. The machined surface flaws are reduced by the transfer of fine equiaxed TiC during cutting. Crush of coarse dendritic TiC particles causes tool coating peeling and adhesion. The additive manufacturing induced microstructure influences machinability (Qiao *et al*. 2022). The machinability of the AMCs was found to be enhanced when TiC and MoS_2 were included in AA7075, as compared to the basic material. Due of the lower ductility with reinforcing TiC and MoS_2 microparticles, the chip shape changes from uninterrupted sheared chips in AA7075 to discrete chips in composite. Because the composites included hard TiC particles, their surfaces were rougher than the base alloy (Dhulipalla *et al*. 2020). ZA37 composites with 5 wt.% and 10 wt.% TiC were made via stir casting, showing enhanced properties. Rising TiC content lowered sample density but increased hardness notably from 131 Hv to 155 Hv. From wear studies, at lower loads, abrasion dominated, shifting to a mix of abrasion and delamination at higher loads. The density was decreased, and the hardness was enhanced when the TiC concentration was increased (Sheikh and Khan, 2025).

A new Minimum Quantity Lubrication (MQL)+LN_2 composite cooling equipment was developed after an analysis of the effects of various injection spots on cooling and lubrication. It was used to investigate the impacts of various cooling techniques on surface roughness, forces, and tool wear of cutting grey cast iron (GCI) and compacted graphite iron (CGI). Cutting CGI and GCI with composite cooling rather than MQL or LN_2 or a mix of the two produced the smoothest surfaces, longest tool life, and least cutting forces, as compared to the other cutting fluids (Meng *et al*. 2024). The effectiveness of Cryo-NMQL in machining of Hastelloy C276 is investigated. Cutting force decreased by 25.49%, cutting temperature by 29.84%, and roughness by 42.50% while using the Cryo-NMQL medium instead of dry cutting. Tool wear diminished by 44.55% with less adhesion and abrasion thanks to this lubricating fluid. Chip morphological examination revealed a less serrated, finer lamella shape with cryo-NMQL (Sen and Bhowmik, 2024). Turning operations on AISI1525 steel was conducted employing Taguchi L_9 arrays under different cooling circumstances by adjusting the machining parameters and simultaneously optimized surface roughness and cutting temperature. Across the board, the experimental trials for surface roughness demonstrated a substantial 68.04% enhancement for the jatropha oil lubricant compared to the mineral oil lubricant. First and foremost, spindle speed accounts for 28.14% of the total output reactions; second, depth of cut accounts for 24.40% (Kazeem and Jen, 2024). During the turning process of EN-24 steel, researchers looked at how different sustainable cooling methods affected the output properties. To produce nanofluids, soluble oils were mixed with nanoparticles of SiC, Al_2O_3, and Al-SiC in various proportions of weight (0.5, 1, and 1.5wt.%). From the perspective of surface excellence, it is recommended to process EN-24 steel in a MQL atmosphere with Al-SiC/soluble oil hybrid NFs using a minimal feed rate along with a rapid cutting speed. By reducing the cutting speed and feed rate, tool wear may be minimized (Thakur *et al*. 2022).

To lower the temperature at the cutting zone during turning of aluminium composites, a variety of lubricating and cooling techniques are used to enhance heat dissipation and reduce tool wear. Flood cooling, cryogenic cooling, MQL and high-pressure cooling are used to direct the coolants directly at the cutting zone (Boothroyd and Knight, 1989). Solid lubricants such as graphite or molybdenum disulfide can be added to the coolant or applied as a coating to the tool, forming a low-friction layer that reduces heat generation. Unlike flood cooling, which requires larger quantity of coolants, MQL uses only a fine mist of lubricant, reducing coolant consumption, operational costs, and environmental impact associated with coolant disposal (Gupta and Davim, 2020). The oil mist in MQL effectively reduces friction and cutting forces at the interface of tool-workpiece, resulting in lower heat production directly at the source rather than relying on coolant to carry it away. This helps improve surface finish quality, minimizes thermal deformation, and prolongs tool life by reducing wear, particularly in abrasive or hard-to-machine materials (Ali *et al*. 2025).

The objective of this research work is to investigate the machining characteristics of aluminium composites, specifically LM25 reinforced with TiC particles, which presents unique challenges due to the hardness and abrasive nature of TiC, which tends to increase tool wear and surface roughness. To overcome this, nano-fluid assisted MQL system was considered to improve the surface integrity with lower tool wear and cutting forces. While considerable research has explored the effects of various coolants and lubrication methods on machining performance, a noticeable gap exists in understanding the specific impacts of MQL when used with uncoated carbide inserts on LM25-TiC composites. Previous studies have often focused on coated tools or alternative lubricants and coolants, leaving limited insight into the performance of uncoated carbide inserts under MQL conditions in this composite context. This gap suggests a novel opportunity to investigate how MQL can influence tool wear, surface finish, and temperature control in machining LM25-TiC composites with uncoated carbide inserts, which may offer cost-

effective and sustainable benefits. The novelty of the present study is to incorporate graphene nanoplatelets (GNPs) in the canola oil to develop and nano-fluid based MQL system which can minimize the adverse effects during turning. Taguchi's technique is adopted for experimental design and the outputs are analysed and optimized with grey relational analysis to identify the most influential parameters and the optimal settings to produces better results.

2. MATERIALS AND METHODS

2.1 Matrix and Reinforcement Material

Aluminium alloy LM25 is used as the matrix which is supplemented with titanium carbide (TiC) 10 wt.%, developed by means of ultrasonic assisted stir casting method. LM25 is an aluminium-silicon alloy valued for its advantageous mechanical qualities, high strength-to-weight ratio, and resistance to corrosion (Govindan and Raghuvaran, 2019). With a density of 2.68 g/cm^3, melting point of 570-580 ℃ and a thermal conductivity of about 155 W/mK, making it suitable for applications requiring efficient heat dissipation. LM25 is commonly used in automotive and aerospace applications, where lightweight and durable materials are essential, as well as in marine environments and heat exchangers, benefiting from its corrosion resistance and thermal conductivity. Titanium carbide is a ceramic material characterized by its high melting point (around 3100℃), excellent thermal stability, and impressive hardness 3000 HV (Srinivasan *et al*. 2024). It has a high modulus of elasticity and outstanding compressive strength, which can enhance the stiffness and load-bearing capacity of aluminium composites. It also possesses a low density of 4.93 g/cm^3, compared to other ceramics. Additionally, TiC offers good thermal conductivity, which helps improve heat dissipation in applications requiring thermal management suitable for high-performance uses in fields including aviation, automobiles, and military (Jiang *et al*. 2017).

2.2 Stir-casting Procedure for Fabrication of Composite

Initially, LM25 alloy is cut into pieces and is heated to a molten state subjected to 750 ℃, to ensure complete melting. Once the alloy is molten, the TiC reinforcements are preheated separately to 300 ℃ to eliminate any surface wetness and to enhance their wettability with the molten aluminium (Upadhyay and Saxena, 2021; Kuttan *et al*. 2024). To achieve a uniform distribution of the nano clay and TiC particles, mechanical stirring at 500 rpm is applied to the melt to further promote uniform particle distribution which improves the connection of matrix to the reinforcements, leading to a more homogenous composite structure. After exhaustive mixing, the molten composite is dispensed into warmed moulds and allowed to solidify, yielding a composite with improved mechanical properties, ideal for high-performance applications requiring lightweight, wear-resistant, and durable materials.

2.3 Taguchi's Approach to Experiment Strategy

Taguchi's technique for designing experiments is a robust method that focuses on improving product quality by optimizing design and manufacturing processes (Taguchi *et al*. 2011; Hisam *et al*. 2024). Developed by Dr. Genichi Taguchi, this technique emphasizes reducing variability in a system's performance, making it less sensitive to external and uncontrollable factors, or noise (Muthukumar *et al*. 2015). Taguchi's approach involves using orthogonal arrays to systematically arrange experiments, allowing researchers to evaluate multiple variables with fewer experiments than traditional methods (Zubair *et al*. 2024). This design strategy enables efficient identification of the most influential factors and their optimal levels, thereby saving time and resources (Senthilkumar *et al*. 2024). In this study, 4 parameters are considered for experimentation with a range of values as given in Table 1.

Table 1. Input settings for experimentation

Parameter	Unit	Notation	-1	0	+1
Cutting Speed	m/min	CS	100	200	300
Feed Rate	mm/rev	FR	0.05	0.1	0.15
Depth of Cut	mm	DoC	0.2	0.4	0.6
Graphene Nanoplatelet	%	GNP	1	3	5

2.4 Grey Relational Analysis

One method under Grey System Theory for analysing connections and determining the level of resemblance or impact across numerous variables is grey relational analysis (GRA), especially when data is incomplete or uncertain (Tzeng *et al*. 2009). It's particularly helpful in decision-making, where it ranks alternatives based on their performance relative to a reference (ideal) sequence. To start, GRA requires normalizing the data to make it dimensionless and comparable (Gunasekaran *et al*. 2024). Normalization is typically done using one of the following equations depending on whether a higher value, lower value, or fixed target is preferred. Let $x_i(k)$ represent the value of the ith sequence at the k^{th} factor or attribute (Omoniyi *et al*. 2024). Higher-is-best normalization,

$$x_i'(k) = \frac{x_i(k) - \min(x_i(k))}{\max(x_i(k)) - \min(x_i(k))} \quad \ldots (1)$$

Lower-is-best normalization,

$$x_i'(k) = \frac{\max(x_i(k)) - x_i(k)}{\max(x_i(k)) - \min(x_i(k))} \quad \ldots (2)$$

A reference sequence x_0 based on the ideal or desired values for each attribute is defined. The normalized value for the reference sequence is denoted as $x_0'(k)$, which is generally the best-performing sequence (e.g., the maximum values for higher-is-better attributes) (Sundara *et al*. 2020).

The grey relational coefficient (GRC) presents the relation amid the reference sequence and each alternative sequence. It is defined as:

$$\xi_i(k) = \frac{\Delta_{min} + \zeta \cdot \Delta_{max}}{\Delta_i(k) + \zeta \cdot \Delta_{max}} \quad \ldots (3),$$

where $\Delta_i(k) = |x_0'(k) - x_i'(k)|$ is the absolute variance amid the normalized reference and alternative values, $\Delta_{min} = \min_{i,k} \Delta_i(k)$ is the smallest value of $\Delta_i(k)$, $\Delta_{max} = \max_{i,k} \Delta_i(k)$ is the largest value of $\Delta_i(k)$, ζ is the distinguishing coefficient, typically set between 0 and 1 (commonly, ζ=0.5) to control the sensitivity. The grey relational grade (GRG) reviews the complete relational degree between the reference and alternative sequences. It's calculated by averaging the GRC for each attribute of a given sequence (Kamis and Acar, 2024):

$$\gamma_i = \frac{1}{n} \sum_{k=1}^{n} \xi_i(k) \quad \ldots (4),$$

where γ_i is the GRG for the i^{th} sequence and n is the number of attributes. The alternatives are ranked based on the GRG γ_i. A higher GRG indicates a closer relationship to the reference sequence, meaning that alternative is more desirable (Shakeri *et al*. 2022).

2.5 Experimental Setup

A computer numeric control-based machining centre is used to turn the workpiece with an uncoated carbide cutting insert of nomenclature CNMG 120404. For each trial a separate workpiece is considered with an insert cutting edge. The workpiece size is Ø10mm of length 150mm. Minimum quantity lubrication setup was attached to the turning centre to provide mist of coolant at the cutting region. The MQL coolant is comprised of canola oil mixed with different weight proportions of GNPs. Canola oil, a base oil that is well-known for its stability, sustainability, and excellent lubricity for GNP dispersion (Sikdar *et al*. 2021). It has excellent biodegradability, superior lubricity, and high thermal stability compared to synthetic and mineral-based lubricants. Its natural ester content provides strong adsorption on metal surfaces, reducing friction and wear more effectively. Canola oil also has a higher flash point, making it safer for high-temperature machining applications. When combined with GNPs, canola oil ensures stable dispersion of nanoparticles. Compared to synthetic and mineral-based oils, canola oil demonstrates superior performance in MQL by offering better wetting characteristics, ensuring uniform lubricant distribution at the tool-workpiece interface. Additionally, its eco-friendly and non-toxic nature makes it a sustainable alternative, reducing health and environmental risks associated with petroleum-based lubricants. This combination of factors makes canola oil a highly effective choice for MQL applications, particularly when paired with GNPs to further enhance machining performance. The addition of GNPs; extremely thin, high-surface-area particles improves canola oil's lubricating and heat-conducting capabilities. To create a stable mixture, GNPs are dispersed in the oil using ultrasonic agitation or mechanical stirring, sometimes with a small amount of surfactant to prevent agglomeration (Banavathu *et al*. 2023). This GNP-enhanced MQL coolant is then applied in precise, minimal amounts to the cutting zone, where it reduces friction, improves heat dissipation, and creates a smoother chip flow. The improved lubricity and cooling effect can help extend tool life, improve surface finish, and reduce energy consumption, making the combination of graphene nanoplatelets and canola oil an efficient, eco-friendly choice for MQL in turning (Khadem *et al*. 2024). The experimental setup used is demonstrated in Fig. 1.

Using GNPs dispersed in canola oil for machining LM25-TiC composites under MQL offers several key benefits, including enhanced lubrication, reduced tool wear, improved heat dissipation, and eco-friendliness. The GNPs, with their ultra-low friction coefficient, form a protective tribofilm at the tool-workpiece interface, minimizing direct metal-to-metal contact and reducing cutting forces. Their excellent thermal conductivity facilitates efficient heat transfer away from the cutting zone, preventing excessive temperature buildup and thermal damage to both the tool and workpiece. Additionally, GNPs exhibit superior mechanical strength, which helps resist abrasive wear caused by the hard TiC particles present in the composite. The use of canola oil as a biodegradable base fluid further enhances sustainability while ensuring effective nanoparticle dispersion. This synergistic combination of GNPs and canola oil in the MQL approach leads to improved machining performance, better surface quality, and extended tool life, making it an efficient and environmentally friendly alternative to conventional lubrication methods. The primary motivation for incorporating GNPs into MQL for machining lies in their exceptional tribological properties, including high thermal conductivity, superior lubricity, and excellent mechanical strength. The GNPs form a protective layer at the tool-chip interface, reducing friction, minimizing tool wear, and enhancing heat dissipation, which leads to improved machining performance and surface quality. This approach distinguishes itself from other lubrication techniques, such as nanofluids containing TiO_2 or MoS_2 nanoparticles, by offering a unique combination of ultra-

low friction and superior thermal management without excessive particle agglomeration or clogging issues commonly associated with spherical nanoparticles. Additionally, graphene's two-dimensional structure allows for effective load distribution and enhanced penetration into the cutting zone, making it particularly advantageous in high-speed and precision machining applications.

3. RESULTS AND DISCUSSION

3.1 Metallography Inference

The fabricated specimen (LM25+10%TiC) *via* stir casting technique was characterized for its microstructure as presented in Fig. 2. Uniform dispersal of TiC particles was seen in the micrograph. This enhances the mechanical strength of the composite. No crack, voids and discontinuities were visualized. This observation was similar to that found by Krishna *et al*. (2022).

3.2 Investigation of Input Parameters

Table 2 presents the input experimental design, and the output performance measures obtained from experiments. Surface roughness was tested using a Mitutoyo Surfboarder SJ1200, while flank wear was examined with a Mitutoyo create tool manufacturers microscope.

Observations from the measured outputs indicate that increasing the cutting speed leads to a significant rise in feed force and surface roughness and a similar trend is observed with an increase in feed rate. At higher CS, the temperature at the cutting region rises significantly, leading to increased friction and thermal stress on the tool (Prvulovic *et al*. 2022). This elevated heat weakens the tool material and promotes faster wear along the flank of the tool, which is a critical area that impacts tool longevity and machining precision. Similarly, an increase in FR elevates the forces exerted on both the tool and workpiece, which results in larger material removal per unit time but also exacerbates the load on the cutting tool (Ercetin *et al*. 2023).

The combined effect of higher CSs and FRs often leads to rougher surface finishes due to the aggressive cutting conditions and pronounced tool wear. The FW and SR tend to lower when the DOC is transformed from 0.2 mm to 0.4 mm, after which a rise in FW and SR is sensed when the DOC is further increased to 0.6 mm. A lower DOC may lead to excessive tool rubbing and increased contact with the workpiece, causing friction-induced wear and a rougher surface (Abellán *et al*. 2024). Conversely, higher DoC amplifies cutting forces and thermal stress, accelerating FW and potentially chipping the tool edge, which further deteriorates surface quality. Thus, an optimal, moderate DOC is crucial in achieving both lower FW and a reduced SR.

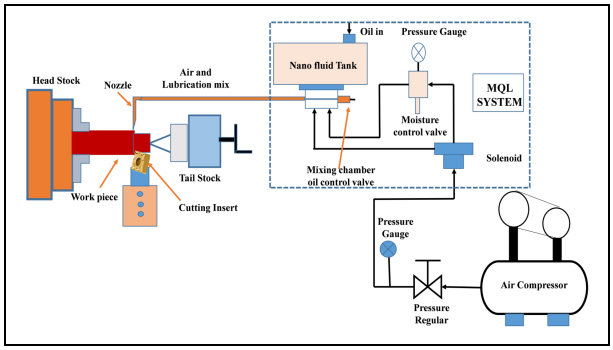


Fig. 1: MQL setup during machining

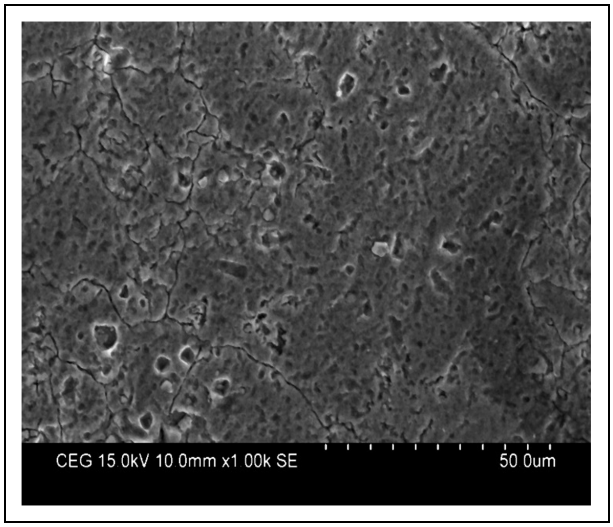


Fig. 2: SEM micrograph of LM25+10%TiC

Table 2. Input array and experimental outputs

Trial No.	Cutting Speed (m/ min)	Feed Rate (mm/ rev)	Depth of Cut (mm)	GNP %	FW (mm)	SR (microns)
1	100	0.05	0.2	1	1.44	1.144
2	100	0.1	0.4	3	1.21	0.966
3	100	0.15	0.6	5	1.78	1.526
4	200	0.05	0.4	5	1.46	1.249
5	200	0.1	0.6	1	1.78	1.136
6	200	0.15	0.2	3	2.45	1.513
7	300	0.05	0.6	3	2.08	1.413
8	300	0.1	0.2	5	2.14	1.551
9	300	0.15	0.4	1	2.72	1.629

The FR and CS significantly affect lubrication performance, influencing both SR and FW. At lower FRs and moderate CSs, the MQL system with GNPs performs optimally, as the lubricant effectively penetrates the tool-

workpiece interface, forming a stable tribofilm that reduces friction and wear. However, at higher FRs, the increased material removal rate leads to higher cutting forces, limiting the lubricant's ability to maintain effective coverage, thereby increasing SR and FW. Similarly, at very high CSs, excessive heat generation can degrade the lubricant film, reducing its effectiveness and accelerating FW. Conversely, at extremely low CSs insufficient heat generation may hinder the activation of lubricating properties of GNPs. A general pattern observed is that moderate CS with low to medium FRs yield the best surface finish and lowest FW, while excessive FRs and CSs lead to deteriorating lubrication performance, resulting in higher SR and accelerated FW.

The inclusion of GNPs in the MQL system enhances the machinability of composite (Altaf *et al.* 2024). The FW tends to lower with higher GNP content in the MQL whereas the SR tends to lower until 3 wt.% addition of GNPs, when the inclusion of GNPs is at 5 wt.%, the SR tends to increase. Inclusion of GNPs in MQL effectively reduces both FW and SR due to their outstanding lubricating capabilities and high thermal conductivity and also creates a protective layer between the tool and workpiece. The GNPs have a high surface area to volume ratio and the developed layer reduces direct contact and friction at the interface, thereby decreasing FW. The high thermal conductivity of graphene also helps dissipate heat more efficiently from the cutting zone, preventing excessive temperature buildup that can accelerate wear and compromise surface quality (Ishfaq *et al.* 2022). The machining performance of LM25-TiC composites under MQL with GNPs peaked at 3 wt.% because this concentration provided the optimal balance between lubrication, thermal conductivity, and dispersion stability. At 5 wt.%, the performance decreased due to excessive GNPs leading to agglomeration, which led to uneven dispersion and clogging at the tool-workpiece interface. This agglomeration reduced the lubricating efficiency, increasing friction and tool wear instead of reducing it. Additionally, an overly thick tribofilm might have disrupted the cutting process, causing instability in chip formation and heat dissipation. Fig. 3 and Fig. 4 present the contour plot showing the influence of input conditions over the FW and SR.

3.3 Multi-criteria Optimization of Outputs

For determining the optimal conditions, GRA is applied, and the procedure is followed. The outputs are tabularized in Table 3. The investigational datasets (outputs) are initially normalized (converting between 0 and 1) for both FW and SR. The next step is to govern the deviation of the normalized value from the ideal value of 1 and subsequently the GRC for FW and SR is determined. Considering equal weightage (50%), the grey relational grade is calculated. The lowest value of GRG is near to black (0) and the higher value is closer to 1 (white) (Anand *et al.* 2022).

By averaging the GRG values corresponding to individual level values of input parameters, the response table for GRG is formulated, as shown in Table 4. From the response table values, main effects plot (Fig. 5) is drawn to identify the ideal conditions which are: CS of 100 m/min, FR of 0.1 mm/rev, DOC of 0.4 mm and 3 wt.% GNP inclusions in MQL system. The impact of CS is higher, shadowed by FR, DOC, and % of GNPs.

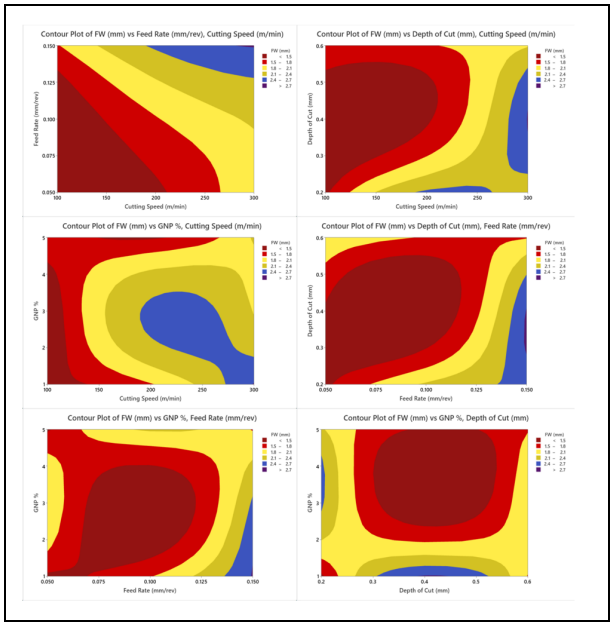


Fig. 3: Variation of FW for the inputs

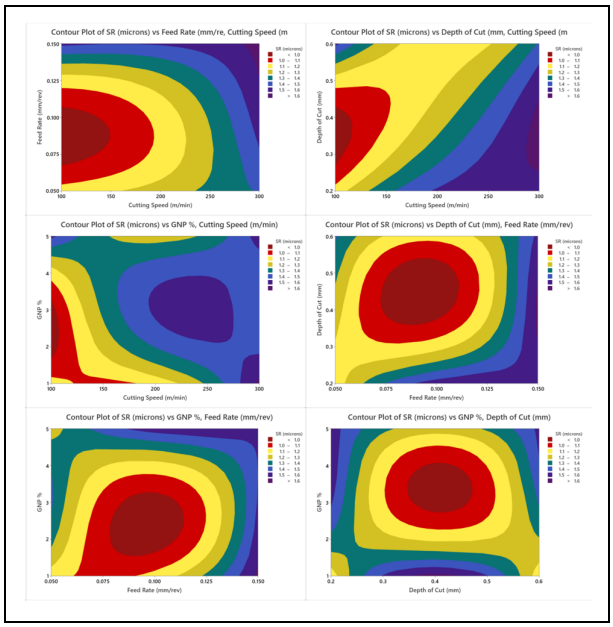


Fig. 4: Variation of SR for the inputs

To identify the influence of combined parameters, interaction plot is drawn as presented in Fig. 6. When two or more factors in an experiment interact, their combined effect on the response differs from the sum of their individual effects. Interaction plots visually

depict these effects by plotting the levels of one factor on the X-axis and showing the response means for each level of another factor, often with lines representing different factor levels (Wakjira *et al*. 2019). There seems to be little to no interaction across the variables if their lines are parallel; if they cross or diverge, it indicates that the factors interact and their effects on the response are dependent on each other (Phadke, 2021).

Among CS and FR, there is considerable interaction for CS of 100 m/min and for a FR of 0.05 mm/rev, whereas for other values, there is no significant interaction. But among CS and DOC and CS and % GNPs there is a considerable relationship which significantly impacts the output responses. When FR combines with DOC and % GNPs, there is a significant interaction and among DOC and % GNP. This clearly illustrates that the combined influence is higher than the individual impact on the output responses.

3.4 Analysis of Variance (ANOVA)

Analysis of Variance is a statistical technique used to analyze experimental datasets to determine the significance of dissimilar factors on a response variable. By partitioning the total variance in the dataset, ANOVA isolates the variability attributed to each factor, distinguishing it from random errors. A high F-ratio indicates a significant effect, suggesting that changes in that factor meaningfully impact the response, a p-value below a pre-determined threshold (often 0.05) confirms that the factor's influence is unlikely due to chance.

The ANOVA table for GRG is presented in Table 5, which shows that the table cannot be formulated as the error degrees of freedom (DoF) is zero. Hence pooling ANOVA desires was done. ANOVA pooling is a technique used to improve the reliability of statistical tests when certain factor effects are deemed statistically insignificant. In ANOVA, each factor or interaction term contributes to the total variance in the dataset. However, when some factors or interactions show negligible influence on the response, pooling combines their mean squares with the residual error term to increase the degrees of freedom for error estimation. This process refines the analysis by reducing random noise and improving the accuracy of the F-ratio for the remaining significant factors (Harrer *et al*. 2021).

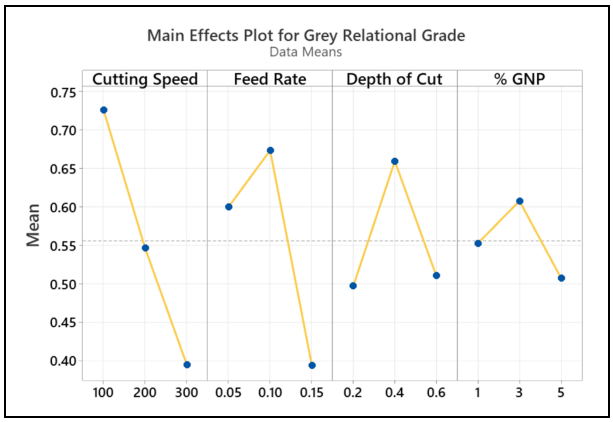


Fig. 5: Main effects plot for GRG

Table 3. GRA table for outputs

Trial No.	Normalizing Sequence		Deviation Sequence		GRC		GRG
	FW	SR	FW	SR	FW	SR	
1	0.848	0.732	0.152	0.268	0.766	0.651	0.709
2	1.000	1.000	0.000	0.000	1.000	1.000	1.000
3	0.623	0.155	0.377	0.845	0.570	0.372	0.471
4	0.834	0.573	0.166	0.427	0.751	0.539	0.645
5	0.623	0.744	0.377	0.256	0.570	0.661	0.615
6	0.179	0.175	0.821	0.825	0.378	0.377	0.378
7	0.424	0.326	0.576	0.674	0.465	0.426	0.445
8	0.384	0.118	0.616	0.882	0.448	0.362	0.405
9	0.000	0.000	1.000	1.000	0.333	0.333	0.333

Table 4. Response table for GRG

Factors	Level 1	Level 2	Level 3	Max - Min	Rank
Cutting Speed	0.726	0.546	0.394	0.332	1
Feed Rate	0.600	0.673	0.394	0.279	2
Depth of Cut	0.497	0.660	0.510	0.162	3
% GNP	0.552	0.608	0.507	0.101	4

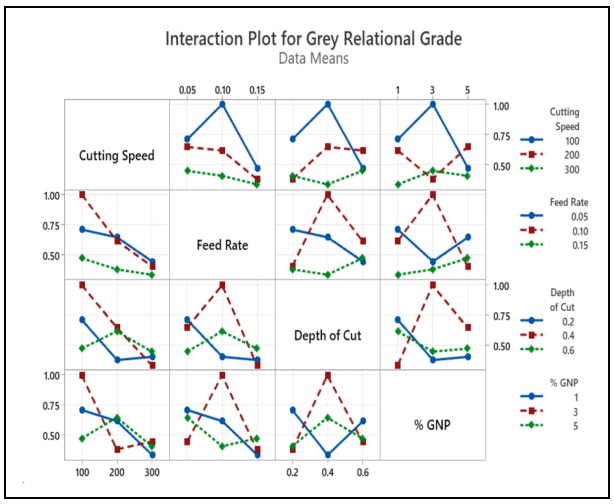


Fig. 6: Interaction plot for GRG

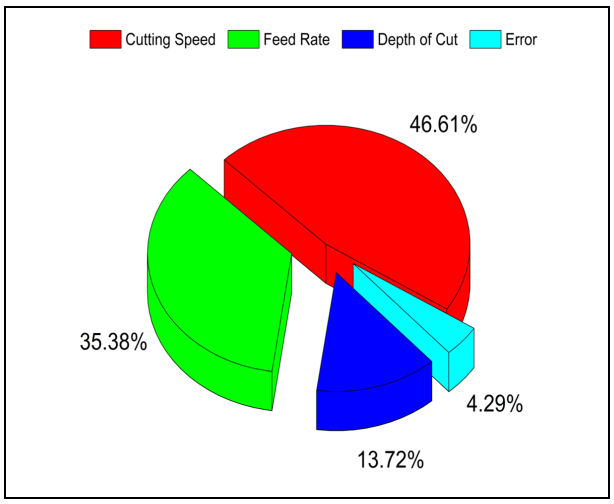


Fig. 7: % Contribution of individual parameters on GRG

Table 5. ANOVA table for GRG

Source	DoF	Adj SS	Adj MS	F-Value	P-Value
Cutting Speed	2	0.16573	0.082864	*	*
Feed Rate	2	0.12582	0.062908	*	*
Depth of Cut	2	0.04879	0.024395	*	*
GNP %	2	0.01525	0.007627	*	*
Error	0	*	*		
Total	8	0.35559			

Pooling serves two main purposes: it strengthens the power of the ANOVA test by estimating the error term better, and it simplifies the model by excluding insignificant terms. This is particularly beneficial in experiments with limited data, as pooling increases the reliability of statistical conclusions (Last *et al*. 2008). The ANOVA table after pooling is presented in Table 6. The insignificant term (% GNP) is combined with the error term and analysis is done. A significant variance exists among all the variables, the F value for CS is higher showing that the influence of CS is maximum than the other input parameters. The R^2 value obtained during analysis is 95.71% with an R^2-adjusted value of 82.84%. The % contribution of each input parameter, excluding the insignificant term (% GNP) is presented in Fig. 7. The CS contributes by 46.61%, FR by 35.38%, DOC by 13.72%, and error term by 4.29% which is within the 95% confidence interval (Bhushan, 2023).

Table 6. Pooled ANOVA for GRG

Source	DF	Adj SS	Adj MS	F-Value	P-Value
Cutting Speed	2	0.16573	0.082864	10.86	0.084
Feed Rate	2	0.12582	0.062908	8.25	0.108
Depth of Cut	2	0.04879	0.024395	3.20	0.238
Error	2	0.01525	0.007627		
Total	8	0.35559			

Fig. 8 presents the tool insert flank face where the wear has occurred which clearly shows that the wear had occurred due to adhesion and delamination owing to increased friction and heat production at the cutting zone as a result of shearing. This observation is similar to that found by Ozkan *et al*. (2020).

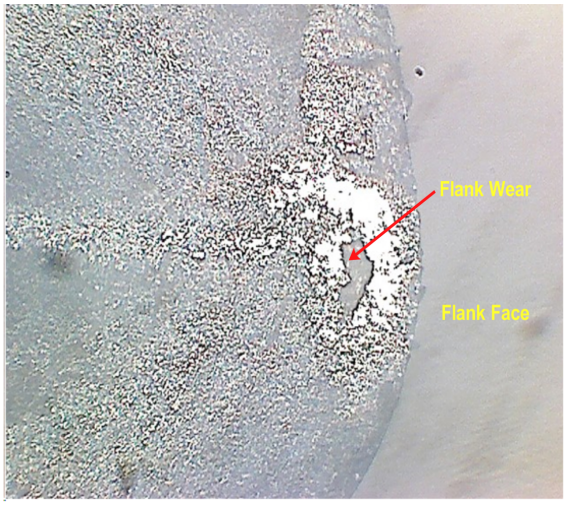


Fig. 8: Flank wear of optimal machining conditions

4. CONCLUSION

This study demonstrates important findings regarding the MQL-assisted machining on the LM25 + 10% TiC composite using GNP-dispersed canola oil. The stir casting technique produced a uniform distribution of TiC particles without defects, as confirmed by SEM analysis, thereby enhancing the mechanical strength of the composite. During turning, increases in cutting speed and feed rate led to a notable rise in feed force and surface roughness, with higher FR further intensifying the forces acting on both the tool and workpiece. The combined effect of elevated CS and FR resulted in rougher surface

finishes due to more aggressive cutting conditions and increased tool wear, while a moderate depth of cut was found to be favorable. The inclusion of GNPs in the MQL system reduced FW, and SR decreased up to an optimal addition of 3 wt.% GNPs, beyond which (at 5 wt.%) SR increased. Multi-objective optimization using GRA identified the optimal machining parameters as a CS of 100 m/min, FR of 0.1 mm/rev, DOC of 0.4 mm, and 3 wt.% GNP inclusion. ANOVA results indicated that CS had the highest contribution (46.61%), followed by FR (35.38%) and DOC (13.72%). Furthermore, significant interactions were observed between CS and DOC, CS and GNP content, as well as between FR and DOC, FR and GNP content, and DOC and GNP content, all of which substantially influenced the machining performance.

FUNDING

This research received no specific grant from any funding agency in the public, commercial, or not-for-profit sectors.

CONFLICTS OF INTEREST

The authors declare that there is no conflict of interest.

COPYRIGHT

This article is an open-access article distributed under the terms and conditions of the Creative Commons Attribution (CC BY) license (http://creativecommons.org/licenses/by/4.0/).



REFERENCES

Abellán, N. J. V., Vila Pastor, C. and Siller, H.R., A Review of the Factors Influencing Surface Roughness in Machining and Their Impact on Sustainability, *Sustainability*, 16(5), 1917 (2024). https://doi.org/10.3390/su16051917

Ali, S. H., Yao, Y., Wu, B., Zhao, B., Ding, W., Jamil, M., Khan, A., Baig, A., Liu, Q. and Xu, D., Recent developments in MQL machining of aeronautical materials: A comparative review, *Chin. J. Aeronaut.*, 38(1), 102918 (2025). https://doi.org/10.1016/j.cja.2024.01.018

Altaf, S. F., Parray, M. A., Khan, M. J., Wani, M. F. and Bhat, F. A., Machining with Minimum Quantity Lubrication and Nano-Fluid MQL: A Review, *Tribol. Online*, 19(3), 209–217 (2024). https://doi.org/10.2474/trol.19.209

Anand, A., Agarwal, M. and Aggrawal, D., Multiple Criteria Decision-Making Methods: Applications for Managerial Discretion, *De Gruyter*, Vol 4, (2022). https://doi.org/10.1515/9783110743630

Atkins, A., The science and engineering of cutting: the mechanics and processes of separating, scratching and puncturing biomaterials, metals and non-metals, *Butterworth-Heinemann/Elsevier*, (2009). https://doi.org/10.1016/C2009-0-17178-7

Banavathu, K. R., Chebattina, K. R. R., Srinivas, V., Moorthy, C. V. K. N. S. N. and Pullagura, G., Physico-chemical and tribological properties of commercial oil – bio-lubricant mixtures dispersed with graphene nanoplatelets, *RSC Adv.*, 13(26), 17575–17586 (2023). https://doi.org/10.1039/D3RA02689B

Bhushan, R. K., Impact of SiC particle size and weight % on tool life while machining of AA7075/ SiC composite, *J. Alloys Metall. Syst.*, 3, 100016 (2023). https://doi.org/10.1016/j.jalmes.2023.100016

Boothroyd, G. and Knight, W. A., Fundamentals of machining and machine tools, 2nd ed. Marcel Dekker, New York, (1989).

Dhulipalla, A., Uday, K. B., Akhil, V., Zhang, J., Lu, Z., Park, H. Y., Jung, Y. G. and Zhang, J., Synthesis and machining characteristics of novel TiC ceramic and MoS2 soft particulate reinforced aluminium alloy 7075 matrix composites, *Manuf. Lett.*, 24, 82–86 (2020). https://doi.org/10.1016/j.mfglet.2020.04.001

Ercetin, A., Aslantaş, K., Özgün, Ö., Perçin, M. and Chandrashekarappa, M. P. G., Optimization of Machining Parameters to Minimize Cutting Forces and Surface Roughness in Micro-Milling of Mg13Sn Alloy, *Micromachines*, 14(8), 1590 (2023). https://doi.org/10.3390/mi14081590

Govindan, K. and Raghuvaran, J. G., Mechanical Properties and Metallurgical Characterization of LM25/ZrO2 Composites Fabricated by Stir Casting Method, *Matér. Rio Jan.*, 24(3), e12439 (2019). https://doi.org/10.1590/s1517-707620190003.0753

Gunasekaran, J., Sevvel, P., John, S. I. and Vasanthe Roy, J., Multi objective optimization of parameters during FSW of AZ80A - AZ31B Mg alloys using grey relational analysis, *J. Mech. Sci. Technol.*, 38(9), 4971–4982 (2024). https://doi.org/10.1007/s12206-024-0832-3

Gupta, K. and Davim, J. P., High speed machining. Elsevier academic press, London, *Academic Press*, (2020). https://doi.org/10.1016/C2017-0-02542-9

Harrer, M., Cuijpers, P., Furukawa, T. A. and Ebert, D. D., Doing Meta-Analysis with R: A Hands-On Guide, 1st edn. Chapman and Hall/CRC, *Boca Raton*, (2021). https://doi.org/10.1201/9781003107347

Hisam, M. W., Dar, A. A., Elrasheed, M. O., Khan, M. S., Gera, R. and Azad, I., The Versatility of the Taguchi Method: Optimizing Experiments Across Diverse Disciplines, *J. Stat. Theory Appl.*, 23(4), 365–389 (2024). https://doi.org/10.1007/s44199-024-00093-9

Huo, D., Chen, W. and Zheng, L., Vibration Assisted Machining: Theory, Modelling and Applications, 1st Ed., *Wiley*, (2021). https://doi.org/10.1002/9781119506348

Ishfaq, K., Maqsood, M. A., Anwar, S., Harris, M., Alfaify, A. and Zia, A. W., EDM of Ti6Al4V under nano-graphene mixed dielectric: a detailed roughness analysis, *Int. J. Adv. Manuf. Technol.*, 120(11–12), 7375–7388 (2022). https://doi.org/10.1007/s00170-022-09207-y

Jiang, M., Zheng, J. W., Xiao, H. Y., Liu, Z. J. and Zu, X. T., A comparative study of the mechanical and thermal properties of defective ZrC, TiC and SiC, *Sci. Rep.*, 7(1), 9344 (2017). https://doi.org/10.1038/s41598-017-09562-x

Raja, K., Senthil, K. M. S., Karthik. A. and Sampath, K. L., Enhancing Drilling Performance in Natural Fiber-Reinforced Biocomposites Using Taguchi Method for Sustainable Manufacturing, *J. Environ. Nanotechnol.*, 13(3), 246–252 (2024). https://doi.org/10.13074/jent.2024.09.243866

Kamis, K. Z. and Acar, Z., Taguchi-Based Grey Relational Analysis on Multiple Damping Characteristics of a Hydraulic Engine Mount, *Arab J. Sci. Eng.,* (2024). https://doi.org/10.1007/s13369-024-09510-8

Kayaroganam, P., Krishnan, V., Natarajan, E., Natarajan, S. and Muthusamy, K., Drilling Parameters Analysis on In-Situ Al/B4C/Mica Hybrid Composite and an Integrated Optimization Approach Using Fuzzy Model and Non-Dominated Sorting Genetic Algorithm, *Metals*, 11(12), 2060 (2021). https://doi.org/10.3390/met11122060

Kazeem, R. A. and Jen, T. C., Performance assessment of Jatropha seed oil as lubricant during turning of AISI 1525 steel using Taguchi-grey relational analysis methodology, *Int. J. Interact. Des. Manuf.,* 18(7)*,* 1-15 (2024). https://doi.org/10.1007/s12008-024-02112-6

Khadem, M., Kang, W. B. and Kim, D. E., Green Tribology: A Review of Biodegradable Lubricants—Properties, Current Status, and Future Improvement Trends, *Int. J. Precis. Eng. Manuf. Green Technol.*, 11(2), 565–583 (2024). https://doi.org/10.1007/s40684-023-00556-x

Krishna, P. S., Dayanand, S., Rajesh, M., Nagaral, M., Auradi, V. and Selvaraj, R., Preparation and Mechanical Characterization of TiC Particles Reinforced Al7075 Alloy Composites, *Adv. Mater. Sci. Eng.*, 20221–11 (2022). https://doi.org/10.1155/2022/7105189

Kuttan, A. A., Rajesh, R. and Anand, M. D., Employing Aluminium Matrix Composite for Stir Casting Process for Investigating the Performance of A1-6061, *J. Inst. Eng. India Ser. D*, 105(1), 395–403 (2024). https://doi.org/10.1007/s40033-023-00469-8

Last, M., Luta, G., Orso, A., Porter, A. and Young, S., Pooled ANOVA, *Comput. Stat. Data Anal.*, 52(12), 5215–5228 (2008). https://doi.org/10.1016/j.csda.2008.04.024

Meng, F., Zhang, Z., Li, J., Li, J., Shi, C., Tian, B., Zhou, H. and Tong, D., A novel approach of composite turning for compacted graphite iron using minimum quantity lubrication and liquid nitrogen jetting by a developed setup, *J. Manuf. Process.*, 117278–288 (2024). https://doi.org/10.1016/j.jmapro.2024.03.021

Muthukumar, V., Suresh Babu, A., Venkatasamy, R. and Senthil, K. N., An Accelerated Particle Swarm Optimization Algorithm on Parametric Optimization of WEDM of Die-Steel, *J. Inst. Eng. India Ser. C*, 96(1), 49–56 (2015). https://doi.org/10.1007/s40032-014-0143-z

Nayak, R. K., Pradhan, M. K. and Sahoo, A. K., Machining of Nanocomposites, 1st Ed., *CRC Press, Boca Raton*, (2022). https://doi.org/10.1201/9781003107743

Omoniyi, P., Acharya, U., Akinlabi, S., Jen, T.-C. and Akinlabi, E., Taguchi-Grey relational analysis driven multi-objective optimization of weld bead geometry and hardness in laser welded Ti6Al4V Alloy, *Int. J. Interact Des. Manuf.,* 19, 423–434 (2025). https://doi.org/10.1007/s12008-024-01880-5

Ozkan, D., Panjan, P., Gok, M.S. and Karaoglanli, A.C., Experimental Study on Tool Wear and Delamination in Milling CFRPs with TiAlN- and TiN-Coated Tools, *Coatings*, 10(7), 623 (2020). https://doi.org/10.3390/coatings10070623

Prvulovic, S., Mosorinski, P., Radosav, D., Tolmac, J., Josimovic, M. and Sinik, V., Determination of the temperature in the cutting zone while processing machine plastic using fuzzy-logic controller (FLC), *Ain Shams Eng. J.*, 13(3), 101624 (2022). https://doi.org/10.1016/j.asej.2021.10.019

Qiao, G., Zhang, B., Bai, Q., Gao, Y., Du, W. and Zhang, Y., Machinability of TiC-reinforced titanium matrix composites fabricated by additive manufacturing, *J. Manuf. Process.*, 76412–418 (2022). https://doi.org/10.1016/j.jmapro.2022.02.033

Sen, B. and Bhowmik, A., Application of minimum quantity GnP nanofluid and cryogenic LN2 in the machining of Hastelloy C276, *Tribol. Int.*, 194, 109509 (2024). https://doi.org/10.1016/j.triboint.2024.109509

Senthilkumar, N., Yuvaperiyasamy, M. and Deepanraj, B., Application of Taguchi design to optimize the operational parameters of pyramid solar still integrated with TiO_2 nanoparticles, *Eng. Res. Express*, 6(4), 045540 (2024b). https://doi.org/10.1088/2631-8695/ad8b0f

Shakeri, Z., Benfriha, K., Zirak, N. and Shirinbayan, M., Mechanical strength and shape accuracy optimization of polyamide FFF parts using grey relational analysis, *Sci. Rep.*, 12(1), 13142 (2022). https://doi.org/10.1038/s41598-022-17302-z

Sheikh, K.A. and Khan, M. M., Predictive modeling of abrasive wear in in-situ TiC reinforced ZA37 alloy: A machine learning approach, *Tribol. Int.*, 202110291 (2025). https://doi.org/10.1016/j.triboint.2024.110291

Sikdar, S., Rahman, M. H. and Menezes, P. L., Synergistic Study of Solid Lubricant Nano-Additives Incorporated in canola oil for Enhancing Energy Efficiency and Sustainability, *Sustainability*, 14(1), 290 (2021). https://doi.org/10.3390/su14010290

Srinivasan, D., Senthilkumar, N., Ganesh, M. and Perumal, G., Characterization studies on nano aluminium composite reinforced with montmorillonite nanoclay and titanium carbide, *Multiscale Multidiscip. Model. Exp. Des.*, 7(3), 2839–2859 (2024). https://doi.org/10.1007/s41939-024-00374-x

Sundara, B. S. R., Ravindran, D. and Moshi, A. A. M., multi-response optimization of CNC turning parameters of austenitic stainless steel 303 using Taguchi-based grey relational analysis, *Trans. Can. Soc. Mech. Eng.*, 44(4), 592–601 (2020). https://doi.org/10.1139/tcsme-2019-0254

Taguchi, G., Chowdhury, S., Wu, Y., Taguchi, S. and Yano, H., Taguchi's quality engineering handbook, *John Wiley Sons* (2011). https://doi.org/10.1002/9780470258354

Thakur, A., Manna, A. and Samir, S., Performance Evaluation of Al-SiC Nanofluids Based MQL Sustainable Cooling Techniques During Turning of EN-24 Steel, *Silicon*, 14(3), 869–882 (2022). https://doi.org/10.1007/s12633-020-00875-7

Tzeng, C. J., Lin, Y. H., Yang, Y. K. and Jeng, M. C., Optimization of turning operations with multiple performance characteristics using the Taguchi method and Grey relational analysis, *J. Mater. Process. Technol.*, 209(6), 2753–2759 (2009). https://doi.org/10.1016/j.jmatprotec.2008.06.046

Upadhyay, G. and Saxena, K. K., Role of Stir Casting in development of Aluminium Metal Matrix Composite (AMC): An Overview, *IOP Conf. Ser. Mater. Sci. Eng.*, 1116(1), 012022 (2021). https://doi.org/10.1088/1757-899X/1116/1/012022

Wakjira, M. W., Altenbach, H. and Perumalla, J. R., Analysis of CSN 12050 Carbon Steel in Dry Turning Process for Product Sustainability Optimization Using Taguchi Technique, *J. Eng.*, 20191–10 (2019). https://doi.org/10.1155/2019/7150157

Zubair, S. W. H., Arafat, S. M., Khan, S. A., Niazi, S. G., Rehan, M., Arshad, M. U., Hayat, N., Aized, T., Uddin, G. M. and Riaz, F., Coupling Taguchi experimental designs with deep adaptive learning enhanced AI process models for experimental cost savings in manufacturing process development, *Sci. Rep.,* 14, 23428 (2024). https://doi.org/10.1038/s41598-024-73669-1